Supplementary Materials

Giant nonlinear optical activityof achiral origin inplanarmetasurfaces with quadratic and cubic nonlinearities

Shumei Chen, Franziska Zeuner, Martin Weismann, Guixin Li, Ventsislav Kolev Valev, Kok Wai Cheah, Nicolae Coriolan Panoiu,* Thomas Zentgraf,* Shuang Zhang*

(I). Measurement of SHG on C4 structures:

By keeping all the other experimental conditions the same, we also measured the SHG from Gammadion-type plasmonic nanostructure with C4 rotational symmetry under pumping power of 60 mW. According to symmetry selection rules of harmonic generation, SHG process on the C4 plasmonic nanostructure is theoretically forbidden for normally incident fundamental wave with circular polarization. However, with imperfection of the fabricated nanostructures used in experiment, the SHG signal from the Gammadion-type nanostructure is not completely eliminated. As shown in **Figure** S1, the circular polarization dependent SHGis measured for fundamental wave with LCP (L) and RCP (R) states. It is observed that the intensity of SHG with RCP (L-R) and LCP (R-L) states are much weaker than that from the C3 nanostructures, despite a stronger pumping power (60 mW for the C4 sample in comparison to 20 mW for the C3 sample).

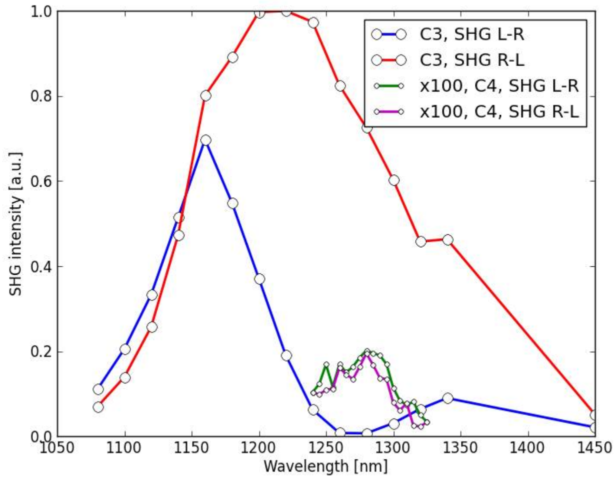

Figure S1: Comparison of SHG spectra between Trisceli- and Gammadion- type plasmonic nanostructures. The pumping power for C3 and C4 nanostructures are 20 mW and 60 mW, respectively. The intensity of SHG from Gammadion-type nanostructure is magnified by 100 times. The measured SHG spectra have opposite circular polarizations (L-R and R-L) as that of the normally incident illuminating light, where the abbreviation of L and R represents for LCP and RCP, respectively.

(II). Calculation of Absolute Value of χ_1 and χ_2:

The effective nonlinear polarization of Trisceli- type nanostructure is defined as:

$$\vec{P}^{2\omega} = (\chi_2 \mp i\chi_1)(\hat{e}_x \mp i\hat{e}_y)\varepsilon_0 E_0^2 \quad . \tag{s1}$$

For the near unity SHG-CD case (wavelength of FW: 1260 nm), χ_1 and χ_2 have the same amplitude and π/2 out of phase. The absolute value of the effective nonlinear polarization can be written as:

$$\left|\vec{P}^{2\omega}\right| = 2\chi_1\varepsilon_0 E_0^2 . \tag{s2}$$

As the effective nonlinear polarization for SHG signal has a linear relationship with the electric field: E_{SHG}, i. e. $\vec{P}^{2\omega} = \chi_0\varepsilon_0 E_{SHG}$, where χ_0 is the linear susceptibility in vacuum. Then, χ_1 can be expressed as:

$\chi_1 = \frac{1}{2}\chi_0 \cdot \frac{E_{SHG}}{E_0{}^2} = \frac{1}{2}\chi_0 \cdot \sqrt{\frac{I_{SHG}}{I_0^2}}$, where $I_{SHG} = 2n\varepsilon_0 E_{SHG}{}^2$ and $I_0 = 2n\varepsilon_0 E_0{}^2$ are the field intensity of SHG signal and fundamental wave, respectively. As we know, $I_{SHG} = P_{SHG}^{av} / R\tau A$ and $I_0 = P_0^{av} / R\tau A$, in which R = 80 MHz, τ = 200 fs and A is the area size of the laser spot. From the measured value of P_{FW}^{av} = 30 mW and P_{SHG}^{av} = 9.33x10^{-8} mW, we finally obtain the absolute value of χ_1 from the following equation:

$$\chi_1 = \frac{1}{2}\chi_0 \cdot \sqrt{\frac{P_{SHG}^{av} \cdot A \cdot R \cdot \tau}{(P_{FW}^{av})^2}} = 5\times 10^{-12} m/V . \qquad \text{(s3)}$$

From the relative ratio (shown in main text) between χ_1 and χ_2, we can also calculate the absolute value of χ_2.

(III). Numerical Simulation of SHG

The SHG calculation is based on linear simulations at the fundamental and second harmonic wavelengths by using COMSOL Multiphysics[1]. Following Ref. 1, the SHG field is given by,

$$E_{nl}(2\omega) \propto \iint \chi_{nnn} E_n^2(\omega) E_n(2\omega) dS \qquad \text{(s4)}$$

where $E_{nl}(2\omega)$ is the SHG signal, χ_{nnn} is the local nonlinear susceptibility, $E_n(\omega)$ and $E_n(2\omega)$ are the linear field normal to the interface calculated at the fundamental and second harmonic frequencies, respectively. The integral is taken over the surface of the nanostructure as the second harmonic generation originates from the interface. Here we call the integrand of s4 as nonlinear contribution, which is a function of the position.

As shown in the plot of amplitude and phase distribution on the bottom surface of the nonlinear contribution (Fig. S2), the strong enhancement is observed at the tips of the Trisceli-type nanostructures.

The origin of nonlinear SHG-CD can be understood from the different field distribution for LCP and RCP incidence, as shown in Fig. S2, and the zoom-in view of the amplitude distribution at a single petal is shown in Fig. S3. It can be seen from the figures that the SHG contribution is concentrated at two edges in each petal, marked as region ‘A’ and ‘B’ in Fig. S3. For both L-R and R-L, the nonlinear contribution in region ‘A’ appears stronger than that in the region ‘B’, and the field in region A and B are approximately out of phase. By interrogating the nonlinear contribution more carefully in Fig. R2, one can see that contribution in region A for R-L is stronger than that for L-R, while contribution in region B for R-L is weaker than that for L-R. Thus, from the distribution of the nonlinear contribution, it is evident that the net contribution, i.e. integration over the whole region, should be stronger for R-L than for L-R due to the difference of phase between region A and B. Note that due to the imperfectness of the computation, the simulation result only agrees qualitatively with the experimental results. The numerical errors are further amplified by the product of the fields in the integration.

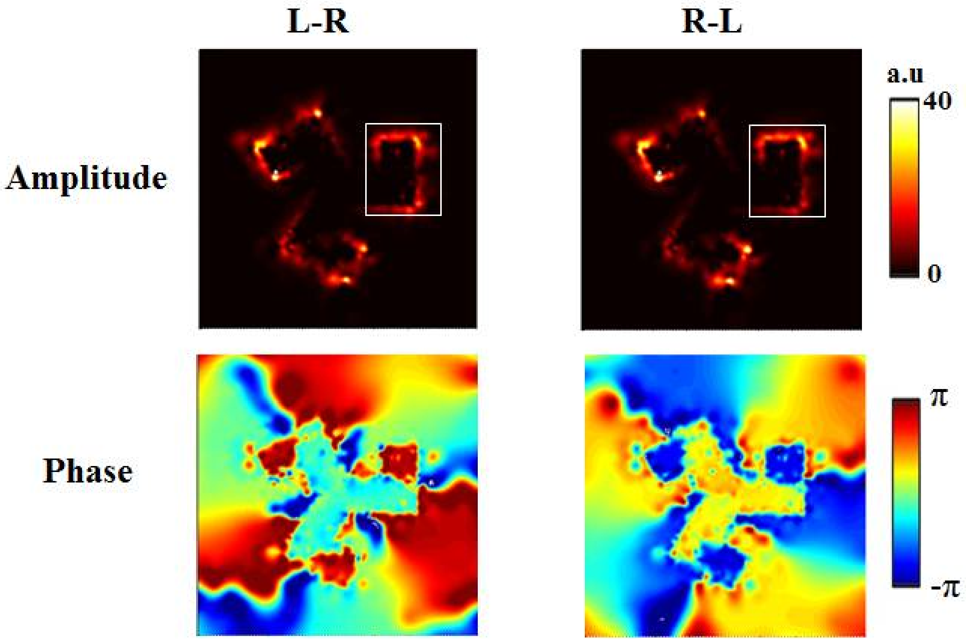

Figure S2. Amplitude and Phase distribution on the bottom surface of $\overrightarrow{f_R} \cdot \overrightarrow{P_L}$ and $\overrightarrow{f_L} \cdot \overrightarrow{P_R}$ (local field contribution to far-field) for left and right circular polarizations at 1291 nm. The first row shows the amplitude distribution while the second row represents the phase distribution.

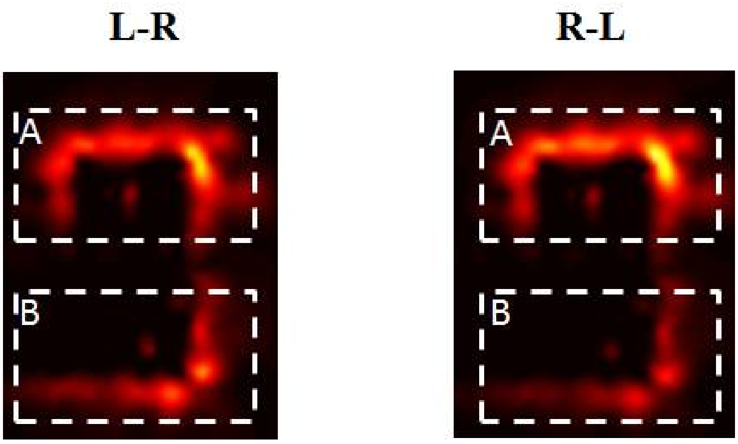

Fig. S3 The zoom-in view of the near field distribution from a single petal.

References:

1. K. O'Brien, H. Suchowski, J. Rho, A. Salandriona, B. Kante, X. Yin, X. Zhang, Nat. Mater. 2015, 14, 379.